THE SHIFTING BASELINE:

Emerging Climate Risk Trends and Parametric Insurance Solutions for Uganda's Smallholder Farmers

Prepared by:
Jonathan Sisa Khabusi

Date:
June 2026

Executive Summary

The agricultural sector operates in a climate that has shifted fundamentally since 2000. This report shows that planting decisions based on accumulated knowledge are becoming dangerously unreliable. Analysing 73 years of climate data and 63 years of crop yield records across Uganda's agricultural zones, it finds that extreme weather events are occurring more frequently and less predictably than before. The seasons farmers plan for are shifting: long rains are arriving later, and in most regions, the likelihood of a severely wet or dry season has almost doubled since the 1980s. Insurance designed around objective, transparent climate data, rather than loss adjustments, is one of the most effective tools available to protect farmers from risks they can no longer reliably predict. This report identifies these risks by zone and proposes a practical framework for parametric insurance products that reflect the trends shaping Uganda's climate.

Figure 1: Map of ZARDIs in Uganda

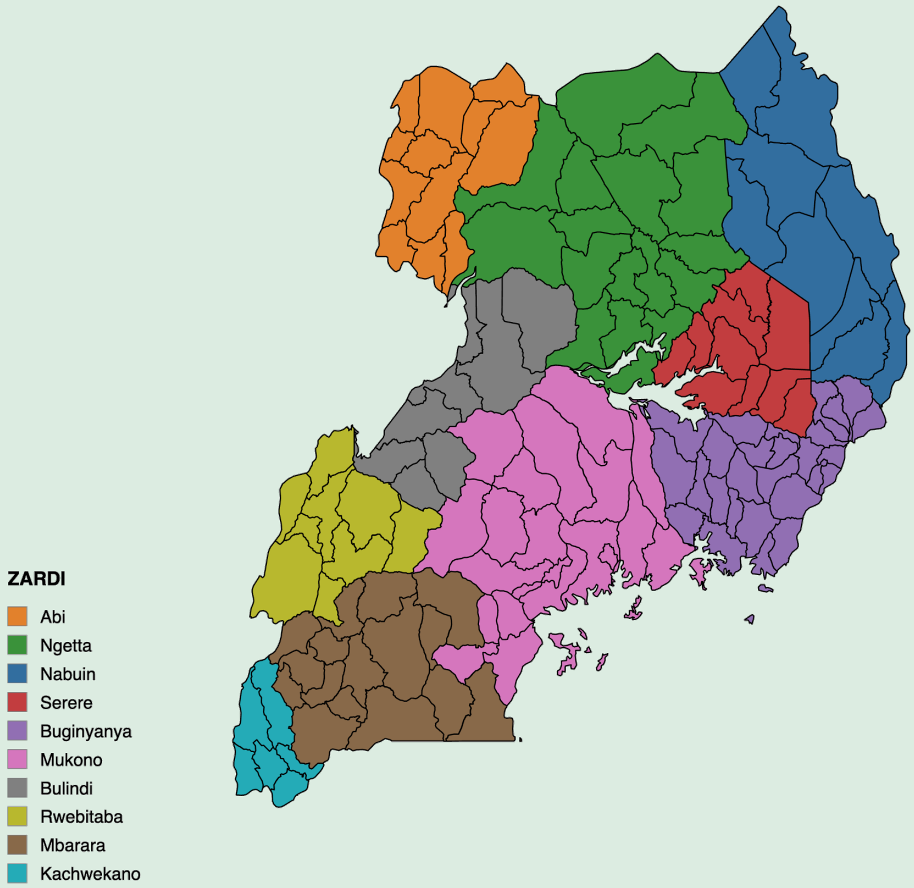

Contents

1 Introduction

1.1 Research Objectives

To analyse 70 years of localised Ugandan weather data to devise climate-smart recommendations of agricultural insurance for Ugandan smallholder farmers. To propose SPEI as a trigger for such products, as temperature or rainfall alone cannot properly convey the intensity of weather events. To highlight which ZARDIs are at the highest risk of climatic shocks to a traditional farmer.

The Office of the Prime Minister (OPM) allocates almost UGX 14 billion annually towards environmental disaster preparedness (OPM Vote Budget Framework, FY2022/23) and is strengthening its capacity to respond to disasters. However, bureaucratic inefficiencies and economic shocks have been proven to reduce this capacity, straining the financial resources of disaster management committees (OPM Strategic Plan). Harnessing the advantages of a partnership with the global insurance industry can mitigate these weaknesses and ensure sustainable development results, in line with Aspiration 1 of Africa's Agenda 2063.

1.2 Background and Context

This report evaluates the climate trajectory over a 73-year horizon (1950–2023) for ten Zonal Agricultural Research and Development Institutes (ZARDIs) responsible for conducting adaptive research within Uganda's agro-ecological zones under the supervision of the National Agricultural Research Organisation (NARO). The ZARDIs include Abi, Buginyanya, Bulindi, Kachwekano, Mbarara, Mukono, Nabuin, Ngetta, Rwebitaba, and Serere. These zones are grouped into districts with similar climatic conditions and soil characteristics, and similar crops are grown accordingly.

Table 1: Principal Crops by ZARDI

ZARDI	Principal Crops Grown
Abi (West Nile)	Sorghum, Finger Millet, Cassava, Green Grams, Cowpeas, Groundnuts
Buginyanya (Eastern)	Maize, Beans, Arabica Coffee, Highland Potatoes, Plantains
Bulindi (Bunyoro)	Maize, Beans, Soybeans, Rice
Kachwekano (Kigezi)	Irish Potatoes, Temperate Fruits (Apples, Pears, Grapes), Barley, Wheat
Mukono (Central)	Robusta Coffee, Bananas, Cocoa
Ngetta (Lango)	Sunflower, Soybeans, Simsim, Cassava, Rice
Nabuin (Karamoja)	Sorghum, Pearl Millet, Sunflower, Mung Beans
Serere (Teso)	Maize, Millet, Sorghum, Beans, Soybeans, Sweet Potatoes, Simsim, Cassava
Mbarara (Ankole)	Bananas (Matooke), Beans, Coffee
Rwebitaba (Tooro)	Tea, Coffee, Bananas, Cocoa

Agriculture contributes tremendously to Uganda's GDP (24.7% in the 2023/24 FY), employs at least 61% of the population (UBOS AS, 2021) and generates foreign exchange through the export of crops such as tea and coffee (UAIS Impact, 2024). As a result of climate change, Uganda's ecosystem is facing intensified rainfall variability, drought, and flood risks. These risks are spatially unequal and increasingly misaligned with historical farmer knowledge. In the Elgon Region, extreme wetness can cause soil erosion, a precursor to landslides in mountainous areas such as Bududa. In the Karamoja region, extreme drought can cause crop loss, despite the dominance of drought-resistant crops.

Agriculture is highly vulnerable to climate risks, making financiers more averse to investing in the sector. Insurance therefore acts as an essential tool for mitigating these risks, enabling farmers to unlock financing opportunities, invest in improved seeds and grow sustainably.

Index-based (parametric) insurance is particularly suited to most smallholder farmers in Uganda. It enhances accessibility by relying on pre-defined triggers, such as rainfall, temperature, or the Standardised Precipitation Evapotranspiration Index (SPEI), verified by third-party data providers, without requiring farmers to confirm actual loss. Unlike traditional insurance, which requires proof of physical damage and time-consuming loss assessments to enable payouts, parametric insurance allows for faster and more cost-effective payouts. Currently, over 1 million farmers are voluntarily seeking coverage despite scepticism, demonstrating its transparency and efficiency in agricultural risk management.

In 2016, the Government of Uganda piloted the Uganda Agricultural Insurance Scheme (UAIS) to cushion farmers from climate shocks and improve access to agricultural financing through subsidised parametric insurance. To date, over UGX 54 billion has been paid out to farmers through the scheme (Africa Agricultural Network, 2026), strengthening farmer resilience and reducing the burden on the OPM during climate-induced disasters.

At the macro level, aggregated risk profiles provide valuable insights for institutions managing regional disaster risk. These profiles categorise risk based on the intensity of the event (e.g., specific rainfall amounts) validated through satellite imagery or ground weather stations. Such information supports disaster risk financing and the design of climate resilience programs (Blue Marble Micro).

1.3 Standardised Precipitation Evapotranspiration Index (SPEI)

The Standardised Precipitation Evapotranspiration Index (SPEI) quantifies the severity of weather conditions using a single numerical value and a corresponding functional risk profile. As a standard normal variable with a mean of 0 and standard deviation of 1, it enables comparison across time, locations and regions. This metric is suitable for applications such as agricultural parametric insurance.

SPEI measures water balance by subtracting Potential Evapotranspiration (PET) from precipitation, indicating the degree of soil moisture deficit or surplus. Its calculation requires only monthly mean temperature and latitude.

Table 2: SPEI Risk Classification

SPEI Value	Category	Agricultural Risk Profile
$\geq +2.00$	Extremely Wet	High risk of flooding; soil saturation
$+1.50$ to $+1.99$	Severely Wet	Drainage issues; moderate flood risk
$+1.00$ to $+1.49$	Moderately Wet	Favourable for water replenishment; low flood risk
-0.99 to $+0.99$	Near Normal	Standard conditions; minimal moisture risk
-1.49 to -1.00	Moderate Drought	Initial moisture stress; potential yield reduction
-1.99 to -1.50	Severe Drought	Significant water shortages; likely agricultural damage
≤ -2.00	Extreme Drought	Severe deficits; high risk of total crop failure

The timescale parameter (k) in this analysis is 3 months. A short-term timescale ($k < 6$) is most suitable for monitoring soil moisture and crop yield. Medium-term timescales ($k = 6$ to 24 months) assess hydrological risks relevant to municipal water supply. Longer timescales ($k > 24$ months) can signal long-term aridification trends.

This risk profiling approach is well-suited to warming climates because it incorporates PET, which captures the atmosphere's evaporating demand even under stable rainfall conditions. The standardisation of the index ensures consistent statistical representation regardless of geographical location (Paulo et al., 2012).

SPEI serves as an operational early warning tool with primary functions including:

- Identifying the onset, duration, and severity of drought events by representing a basic climatic water balance.
- Providing insight into the effects of increasing or decreasing pressure on water resources.
- Triggering early warnings based on defined thresholds (e.g., values below −2.0 indicate extreme drought).
- Being projected using General Circulation Models (GCMs) outputs to support long-term climate resilience and policy planning.

2 Descriptive Analysis of Ugandan Climate

Uganda has a tropical climate characterised by bimodal rainfall, with wet seasons from March to May (MAM) and September to November (SON), separated by dry seasons from December to February (DJF) and June to August (JJA). Rainfall peaks typically occur in April and October.

Rainfall commonly declines after November and remains below the 100mm threshold for planting between December and February, except in Kachwekano, Buginyanya, Rwebitaba, and Mukono. These ZARDIs support year-round cropping due to relatively consistent rainfall. For many staple crops, such as maize, a minimum of 100mm of monthly rainfall is required to achieve viable yields. Maintaining stable crop production is critical for both food security and economic stability, given that external agricultural shocks pose significant macroeconomic risks to Uganda's GDP. For example, the 2010/11 severe drought led to an estimated 1.8% reduction in GDP growth (Agricultural Risk Assessment Study 2015, Section 4.2.2).

Annual rainfall variability is high across most regions. Monthly rainfall in April, for instance, could reach 350mm, over 100mm above the average. Buginyanya and Rwebitaba exhibit particularly high variability, with coefficients of variation (CVs) exceeding 64%, signalling unpredictable rainfall patterns. In contrast, temperature variability is relatively low. Northern and central regions such as Serere, Ngetta and Mukono have CVs below 5%, indicating stable temperature conditions year-on-year.

Most regions follow a clear bimodal rainfall pattern, with peaks during April–May and October–November, and a dry period between June and August (JJA). However, Nabuin is an exception, exhibiting a unimodal rainfall pattern with higher rainfall in June and July and a single planting season from April to September (FAO, 2025).

Mean temperatures across most regions range between 20°C and 25°C. Warmer conditions are observed in Abi, Ngetta, Nabuin, and Serere, while cooler regions such as Rwebitaba, Buginyanya, Mbarara, and Bulindi typically peak around 20°C. Kachwekano stands out with temperatures consistently below 20°C due to its elevated topography (1,262–3,883 m above sea level).

Buginyanya consistently records significantly higher monthly rainfall, with four months exceeding 300 mm on average. In contrast, Mbarara experiences lower rainfall peaking between 150–180 mm, with monthly rainfall declining sharply to approximately 50–80 mm during JJA. A dry month is typically defined as receiving less than 50mm of rainfall, while a wet month exceeds 100 mm. Areas prone to drought are typically in the 'Cattle Corridor', which is more suitable for livestock rearing than crop cultivation. Regions such as Mbarara and Nabuin, with relatively low annual rainfall, align with this classification. (World Bank Climate Risk Profile, 2025).

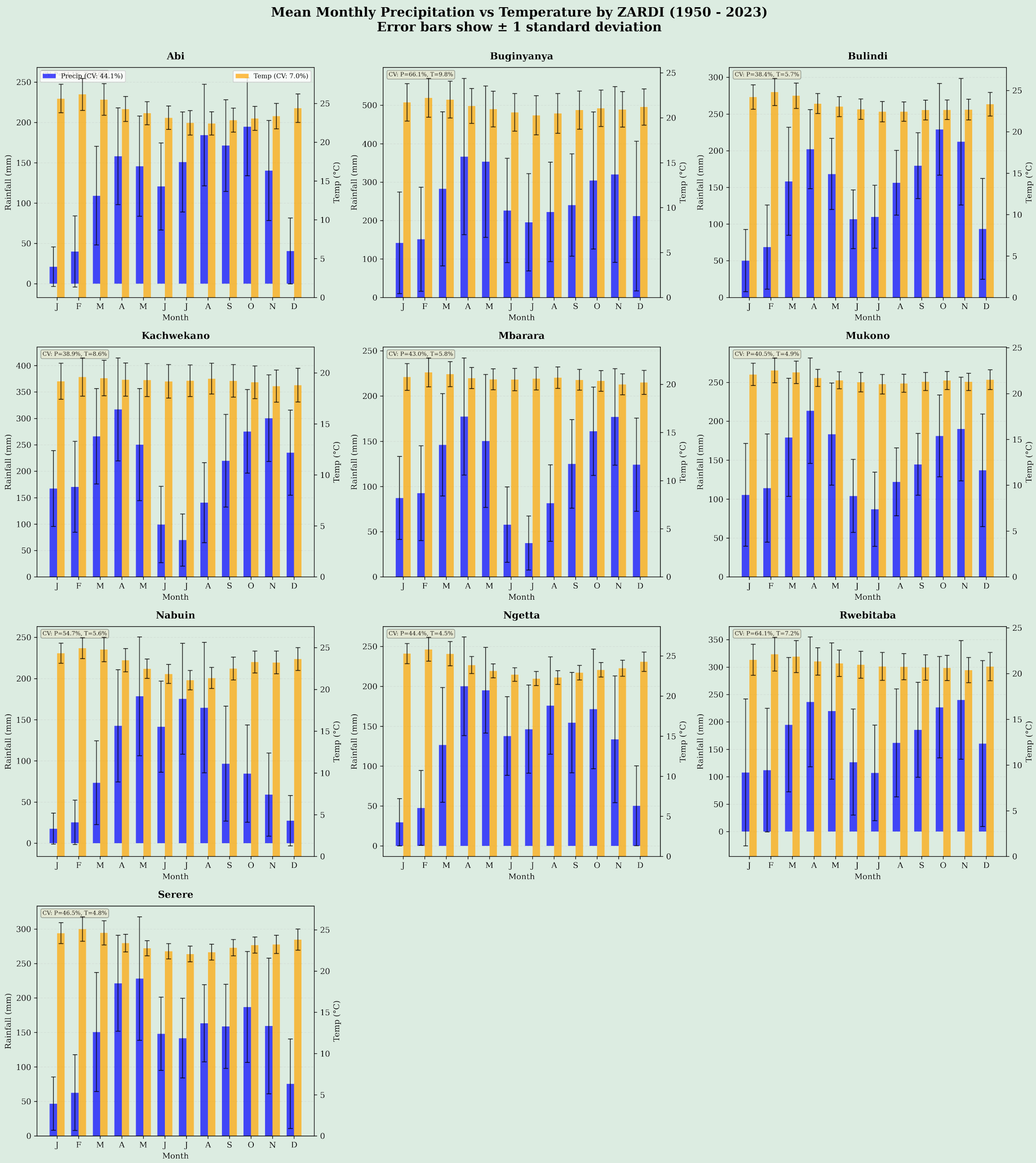

Figure 2: Mean Monthly Rainfall and Temperature by ZARDI

2.1 Rainy Season Onset Analysis

The onset analysis investigates whether the timing of seasonal rainfall onset is shifting across Uganda's ZARDI regions. The onset date defines when planting conditions become viable, and temporal shifts directly affect index trigger calibration, payout timing, and basis risk. The analysis targets both MAM (long rains) and SON (short rains) seasons.

The table below presents Mann-Kendall (MK) trend test results for seasonal onset timing across the ten ZARDIs.

Table 3: Mann-Kendall Trend Test Results for Seasonal Onset

	SON					MAM				
ZARDI	n	τ	p-value	Trend	*Sig	n	τ	p-value	Trend	*Sig
Abi	38	−0.016	0.8421	–	F	37	−0.026	0.7447	–	F
Buginyanya	40	**−0.127**	**0.0136**	**decrease**	T	38	−0.129	0.0728	–	F
Bulindi	38	0.010	0.9152	–	F	37	−0.110	0.1883	–	F
Kachwekano	39	0.004	0.9755	–	F	36	0.037	0.6619	–	F
Mbarara	42	0.136	0.0781	–	F	40	−0.072	0.2885	–	F
Mukono	39	−0.046	0.6277	–	F	37	−0.075	0.4252	–	F
Nabuin	39	−0.150	0.1631	–	F	44	**−0.217**	**0.0063**	**decrease**	T
Ngetta	38	−0.104	0.2396	–	F	40	**−0.158**	**0.0273**	**decrease**	T
Rwebitaba	40	−0.042	0.6519	–	F	36	−0.100	0.2422	–	F
Serere	35	−0.086	0.3295	–	F	38	−0.100	0.2360	–	F

**significance flag (True or False) at* $\alpha = 0.05$

Most ZARDIs do not exhibit statistically significant trends in seasonal onset, suggesting that average onset timing has remained broadly stable over 1950–2023. However, three negative trends are observed, concentrated in northern and eastern Uganda.

During SON, Buginyanya shows a decreasing trend ($\tau = -0.127$), suggesting a shift towards delayed or less reliable short rains. In the MAM season, Nabuin ($\tau = -0.217$) and Ngetta ($\tau = -0.158$) were the only ZARDIs with significant negative trends. For Nabuin, a decreasing MAM trend is particularly critical because this unimodal region has only one planting season, meaning a delayed onset reflects a drying pattern at the start of the rainy season, directly constraining planting opportunities.

2.2 Seasonal Risk of Extreme Events

Using aggregated monthly SPEI values, a running cumulative sum is applied to identify extreme events by thresholds of $+2.0$ (extreme wetness) and -2.0 (extreme drought). This approach reduces noise from normal seasonal variability. Once an extreme event is detected, persistence within the extreme threshold over the subsequent three months is verified. Non-persistent events are excluded.

Table 4: Frequency of Extreme Seasonal Anomalies by ZARDI and Decade

	1950				1960				1970				1980				1990				2000				2010				2020*			
	Dry		Wet		Dry		Wet		Dry		Wet		Dry		Wet		Dry		Wet		Dry		Wet		Dry		Wet		Dry		Wet	
ZARDI	M	S	M	S	M	S	M	S	M	S	M	S	M	S	M	S	M	S	M	S	M	S	M	S	M	S	M	S	M	S	M	S
Abi	9	4	0	0	6	3	0	0	6	3	0	1	2	1	2	1	1	0	4	1	0	0	9	2	0	0	7	2	0	0	3	1
Buginyanya	5	1	0	1	6	3	0	0	4	4	0	0	3	1	1	0	3	1	0	0	8	2	8	2	1	0	7	2	1	0	3	0
Bulindi	7	1	0	0	6	4	0	0	6	5	0	0	3	2	2	0	2	0	4	2	0	0	8	2	0	0	8	4	0	0	3	3
Kachwekano	7	0	0	1	7	2	0	1	8	3	0	1	2	1	2	0	1	0	4	1	0	0	7	3	0	1	8	1	0	0	3	0
Mbarara	8	0	0	0	7	3	0	0	8	4	0	0	3	1	3	0	1	0	4	0	0	0	10	4	0	1	8	3	0	0	2	1
Mukono	8	1	0	0	7	2	0	0	7	4	0	0	3	1	1	0	2	0	3	0	0	0	9	2	0	0	8	2	0	0	3	3
Nabuin	8	3	0	0	6	1	0	0	4	2	1	0	1	1	1	2	1	1	5	2	0	0	6	2	2	0	5	1	1	1	3	1
Ngetta	8	1	0	0	7	3	0	0	6	3	0	1	2	2	2	0	2	0	4	1	0	0	8	2	1	0	7	3	0	0	3	1
Rwebitaba	6	0	0	0	7	2	0	1	8	4	0	1	2	1	2	0	2	0	4	1	0	0	8	2	0	1	8	1	0	1	2	1
Serere	8	1	0	0	7	3	0	0	5	3	0	0	2	1	1	0	2	1	4	1	0	0	8	2	1	0	7	2	0	0	3	0

**2020s data covers only four years.*

Analysis of MAM anomalies reveals a transition beginning in the 2000s, shifting from a drought-dominated climate to one increasingly characterised by extreme wetness. Between 1950 and 1980, each ZARDI experienced 5–9 droughts per decade during MAM. From 2000 onwards, extreme wet events became more frequent, with 5–10 occurrences per ZARDI per decade. Although the 2020s dataset is incomplete, over half of observed MAM seasons (2–3 out of 4) continue to exhibit extreme wetness. This trend points to rising risks of crop loss from waterlogging and soil saturation, especially in Abi, Mbarara, Bulindi, and Mukono.

In contrast, SON anomalies show a weaker transition from extreme drought to extreme wetness over time. Both extreme drought and wet events occur less frequently, and the shift towards wetness is less pronounced compared to the MAM season.

2.3 Severe Wetness Risk

Using SPEI, the 2020s exhibit a clear increase in the frequency of severe wetness relative to previous decades, with Mukono standing out as particularly exposed. In agricultural systems, excess moisture can be as damaging as drought.

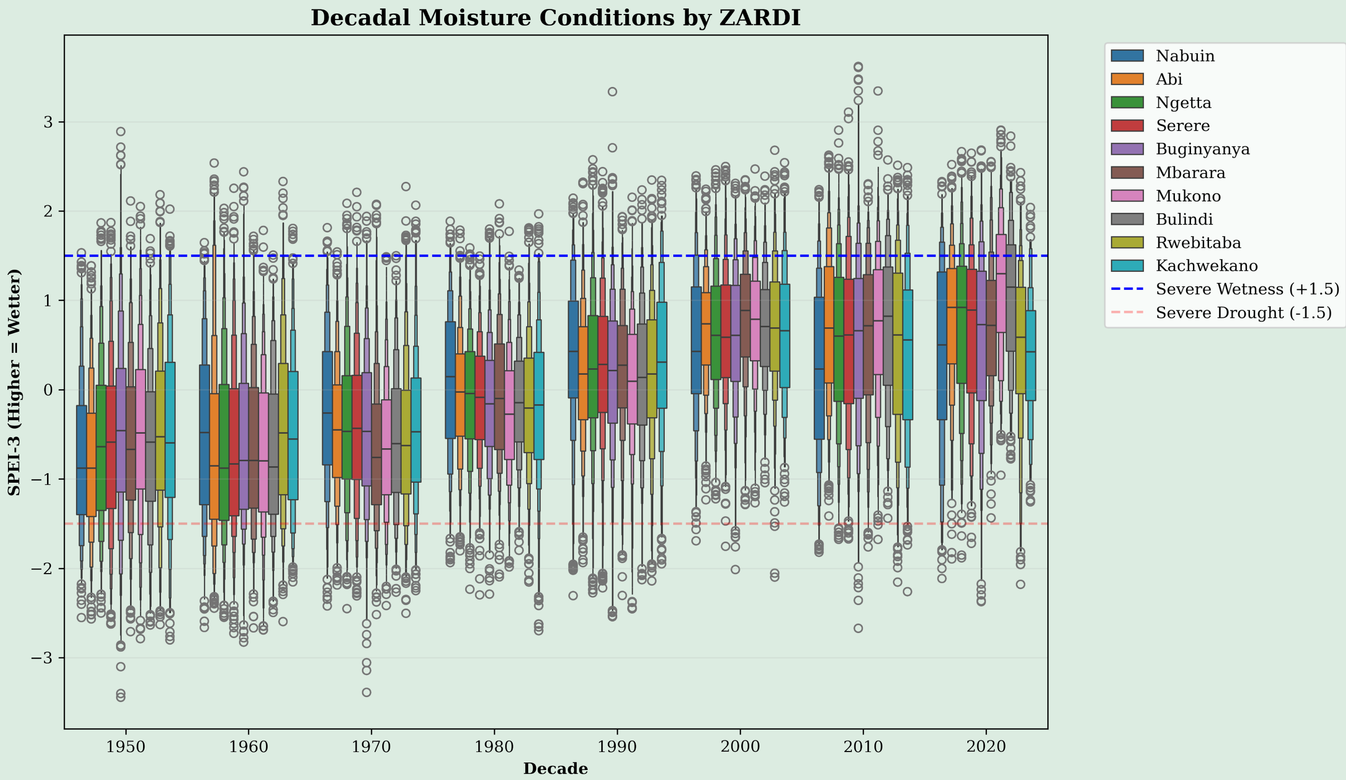

Figure 3: Regional distribution of SPEI anomalies across Ugandan ZARDIs, showing extreme outliers.

This shift is reflected in the upward movement of the median line over time. From the 1950s to the 1970s, median values hovered slightly below zero. By the 2010s and 2020s, medians across most ZARDIs have shifted closer to $+1.0$, signalling a wetter baseline. This indicates a structural shift in flood risk. However, this transition is spatially uneven: ZARDIs such as Mukono, Bulindi, and Abi show the most pronounced movement in median SPEI, while western regions like Kachwekano and Rwebitaba remain closer to their historical baselines. This divergence highlights the importance of location-specific risk assessment, as uniform flood risk pricing would fail to capture these regional differences.

At the same time, distributional changes point to increasing variability. Despite rising medians, lower tails have lengthened across decades. Buginyanya consistently exhibits particularly long lower tails, where deep drought extremes coexist alongside elevated medians. In the 2020s, observations exceed both -2.0 and $+2.5$, reflecting a widening spread where the same decade contains both the wettest and driest conditions in the record.

2.4 Increasing Unpredictability

In the 1970s and 1980s, most observations fell within the $[-1.5, +1.5]$ band, the predictable farming zone. By the 2010s and 2020s, wider distributions emerge, with a growing proportion of observations lying outside this range, reflecting increased frequency of both severe wetness and severe drought.

Using aggregated SPEI values by decade, climate volatility is defined as the proportion of observations exceeding an absolute threshold of 1.5.

Table 5: Climate Volatility (%) by ZARDI and Decade

ZARDI	1950	1960	1970	1980	1990	2000	2010	2020*
Abi	21.0	29.9	7.0	2.0	6.0	7.9	21.4	18.8
Buginyanya	20.3	17.3	11.4	2.2	7.7	11.7	17.4	20.6
Bulindi	19.5	19.0	12.7	1.5	6.5	10.2	19.8	31.7
Kachwekano	19.3	16.9	12.1	6.5	14.2	14.6	15.2	7.3
Mbarara	15.6	19.2	18.0	2.2	5.8	15.0	18.3	13.9
Mukono	17.6	18.8	11.9	2.6	3.8	11.8	18.4	39.0
Nabuin	20.5	18.1	8.1	4.0	13.6	13.0	12.8	24.7
Ngetta	20.8	25.0	11.0	1.4	9.4	11.6	17.7	20.1
Rwebitaba	16.2	17.7	14.9	4.9	7.9	15.1	20.7	13.1
Serere	20.6	21.1	11.9	1.1	8.1	11.2	18.0	18.0

**2020s data covers only four years.*

The 1980s were the most stable across all ZARDIs, with average volatility of 2.8%. From the 2010s onwards, most regions exhibit an upward trend, peaking in the 2020s for Buginyanya, Bulindi, Mukono, and Nabuin. Mukono records the highest volatility in the 2020s at 39%, followed by Bulindi at 31.7%. Kachwekano displays the lowest volatility at 7.3%, close to its historical low of 6.5% observed during the stable 1980s.

2.5 Increasing Dual-Peril Risk

Drought and flood insurance can no longer be designed or priced as separate products for certain climate risk profiles. Within a single decade, the same ZARDI can experience both drought and flood conditions severe enough to trigger payouts. During the 2010s, the upper tail exceeded SPEI $+3.0$ while the lower tail fell below -2.0.

A drought-only trigger (e.g. SPEI < -1.5) would leave farmers exposed to increasingly significant flood risk. This highlights the need for dual-trigger insurance products that pay out when SPEI exceeds +1.5 for sustained wet conditions or falls below -1.5 for drought. These findings also point towards rising basis risk, especially in the eastern ZARDIs, where variability is increasing most rapidly.

Extreme outliers in the 2010s were influenced by the 2015–2016 El Niño event, during which East Africa experienced one of its wettest El Niño seasons on record (MacLeod et al., 2019).

3 Impact of ENSO & IOD in Uganda

3.1 El Niño/La Niña (ENSO)

Under normal conditions, trade winds over the eastern tropical Pacific Ocean blow westward along the equator. El Niño disrupts this pattern by warming the Pacific Ocean surface waters. This warming lowers atmospheric pressure above the ocean and reverses typical air circulation. It is often followed by La Niña, which is characterised by unusually cool ocean surface temperatures. Together, these phenomena form the oceanic component of El Niño-Southern Oscillation (ENSO) (National Geographic, 2025). The strength and phase of ENSO is determined using the Relative Oceanic Niño Index (RONI).

In Uganda, El Niño is generally associated with above-average rainfall, increasing the risk of flooding. In contrast, parts of Southern Africa, including Zambia, Zimbabwe, Malawi, and South Africa, often experience droughts and heat waves during El Niño events. The 2023–2024 El Niño was more pronounced than the 2015–2016 event, affecting more countries (UNOCHA, 2024).

The overall ENSO cycle is projected to become more frequent and intense due to climate change, amplifying both wet and dry extremes across affected regions (Malteser International, 2026).

3.1.1 Trends and Intensification of El Niño Impacts Across Decades

Global El Niño events occurred in 1957–58, 1963–64, 1965–66, 1972–73, 1982–83, 1986–87, 1991–92, 1997–98, 2002–03, 2009–10, and 2015–16. More recent events are associated with a greater risk of severe wetness. During the 2015–2016 event, all ZARDIs crossed the SPEI threshold of $+1.5$.

In the two earliest periods shown, SPEI distributions during El Niño events were relatively contained. In contrast, the 2015–2016 event shows far more pronounced outliers, especially in Buginyanya, Mukono, and Serere. A comparison across decades also shows a clear increase in the interquartile range (IQR). This expansion is more pronounced in eastern ZARDIs such as Buginyanya and Serere compared to western ZARDIs such as Mbarara and Bulindi.

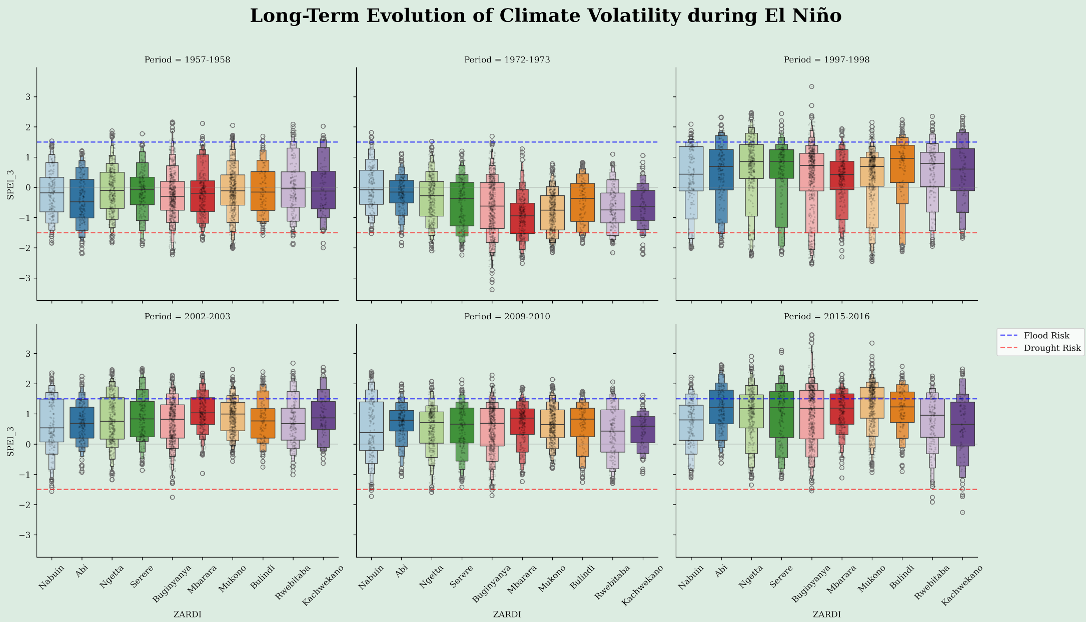

Figure 4: Regional distribution of SPEI during El Niño

The wetting signal associated with El Niño is therefore clear, though spatially uneven. By 2015–2016, median SPEI values are close to $+1.0$ in Buginyanya, Abi, Ngetta, Mukono, and Serere, suggesting that even typical El Niño conditions in these zones are now moderately wet. The upper tail extends more strongly than the lower tail contracts, indicating that El Niño primarily amplifies wetness risk in Uganda.

3.1.2 Patterns and Impacts of La Niña Across Decades

Global La Niña events occurred in 1955–56, 1973–74, 1988–89, 1998–99, 2007–08, 2010–11, and 2016–17 (Golden Gate Weather Services, 2026). La Niña is typically associated with below-normal rainfall in Eastern Africa, often resulting in severe drought conditions across the Greater Horn of Africa, including Kenya and Somalia. Consistent with these expectations, SPEI values fall below severe drought thresholds. However, the 2016–2017 event includes instances of severe wetness, indicating a weaker drought signal, potentially influenced by preceding El Niño-induced moisture conditions.

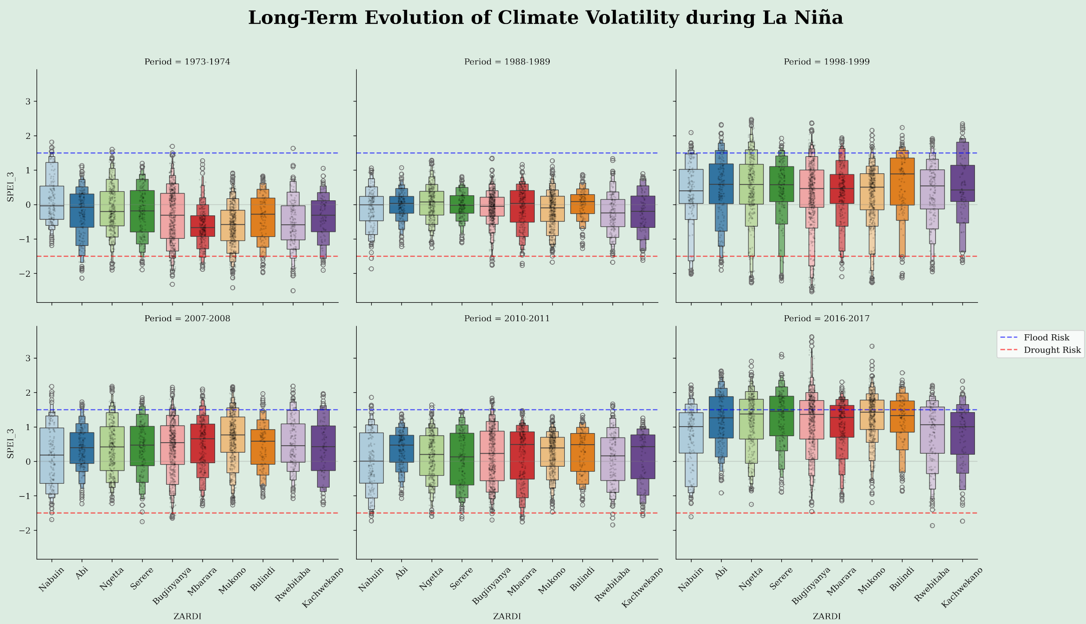

Figure 5: Regional distribution of SPEI during La Niña

Early La Niña periods, such as 1988–1989, are characterised by relatively narrow SPEI distributions. More recent events such as 2010–2011 and 2016–2017 display notably longer upper and lower tails. The 2016–2017 La Niña period stands out with some of the highest median SPEI values observed across the entire La Niña record. This event is anomalous, as it was marked by severe wetness despite the typical dryness associated with La Niña. By comparison, the 2010–2011 panel shows more moderate expansion in the IQR, suggesting that the rising variability of La Niña events is driven by compound events rather than a smooth, gradual trend. This contrasts with El Niño, where increases in variability appear more consistent over time.

In both 1998–1999 and 2016–2017, median SPEI values in several ZARDIs approach $+1.0$, coexisting with extended lower tails towards the -1.5 drought threshold. This pattern reflects climatic 'whiplash', where overall wet conditions mask the simultaneous occurrence of severe, short-lived drought episodes. Western ZARDIs such as Kachwekano and Rwebitaba tend to show lower median SPEI, suggesting greater exposure to the drying component of La Niña.

3.1.3 Severity During El Niño

To assess the severity of El Niño, months with SPEI values above +1.5 or below -1.5 are classed as severe. The heatmap below shows the percentage of severe months during each El Niño event across the ZARDIs.

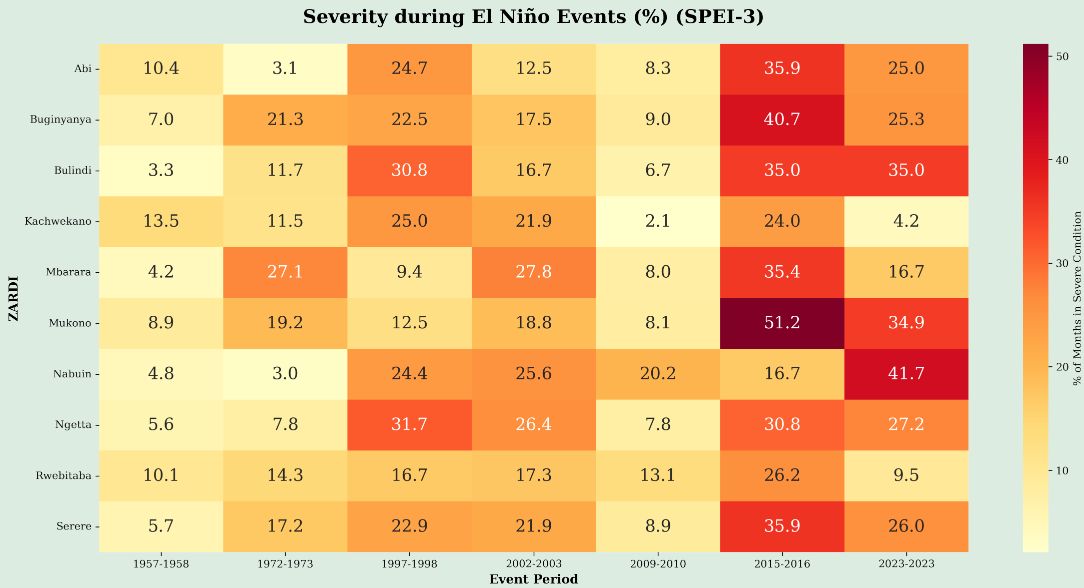

Figure 6: El Niño Severity by ZARDI

The results show that ENSO affects Uganda unevenly. The 2015–2016 El Niño event stands out as the most severe in the record. Western zones such as Rwebitaba, Mbarara, and Kachwekano show lower severity during El Niño, while eastern regions such as Buginyanya, Bulindi, Serere, and Nabuin are more affected. Mukono shows the most severe conditions during the 2015–2016 El Niño and ranks among the most severe again in 2023.

Regions experiencing frequent severe months during El Nino should monitor such signals closely for better risk management.

3.1.4 Seasonal Severity During El Niño

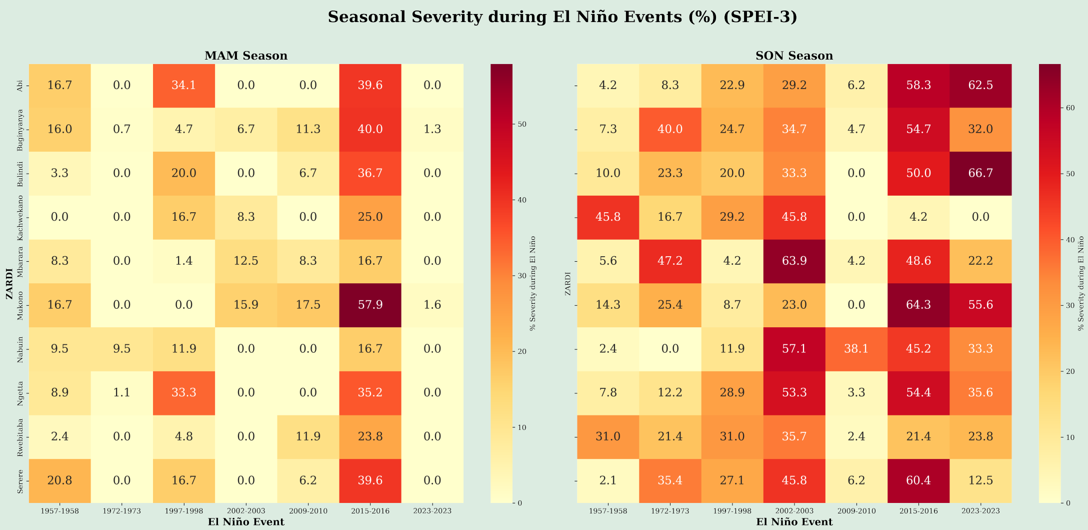

Figure 7: El Niño Seasonal Severity by ZARDI

El Niño generally has a greater impact during SON than during MAM. This seasonal contrast is explicitly illustrated in 2023, when more severe conditions occurred during SON than during MAM, consistent with the fact that El Niño was officially declared by NOAA in June, after the MAM season had ended.

3.2 Indian Ocean Dipole (IOD)

The Indian Ocean Dipole (IOD) is a key driver of climate variability across the Indian Ocean, operating independently of ENSO. It reflects sea surface temperature (SST) anomalies coupled with changes in atmospheric convection (JMA, 2002). The strength and phase of the IOD is determined using the Dipole Mode Index (DMI).

The IOD is classified into three distinct phases: a positive phase (DMI $> +0.4$), a negative phase (DMI < -0.4), and neutral (-0.4 to $+0.4$). Non-neutral IOD events typically develop around May or June, intensify through mid-year, and peak between August and October before dissipating by November. As a result, the MAM season generally coincides with a neutral IOD phase.

During negative IOD events, stronger westerly winds lead to cooler waters in the western Indian Ocean, reducing moisture availability and contributing to drier conditions. Conversely, positive IOD events are associated with warmer waters in the western Indian Ocean, enhancing moisture transport and increasing rainfall over East Africa (Australian Bureau of Meteorology).

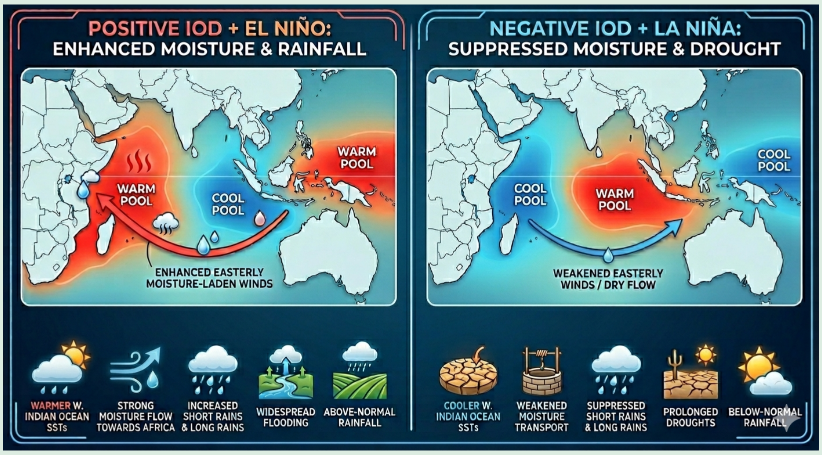

Figure 8: Infographic illustrating positive and negative IOD phases, detailing their contrasting impacts on East African rainfall

3.2.1 Analysis of SPEI Extrema During Indian Ocean Dipole Events

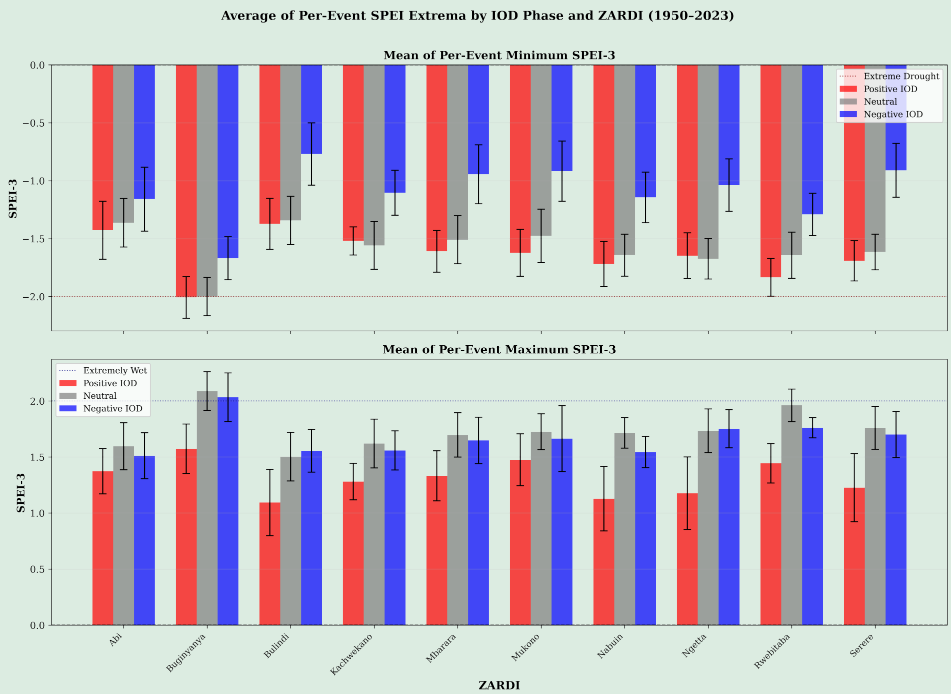

Figure 9: Aggregated SPEI Extrema categorised by IOD phase

Figure 9 presents the average extreme SPEI recorded for each ZARDI during positive, negative, and neutral Indian Ocean Dipole (IOD) phases. By focusing on the maximum and minimum SPEI values observed during each event, the analysis highlights the intensity of severe wet or dry conditions across regions.

The results show that negative IOD events are associated with higher average SPEI values, indicating more intense wet conditions, while positive IOD events correspond to lower SPEI values, reflecting more severe dry conditions. Interestingly, neutral IOD events also exhibit a relatively high severity of wetness across all ZARDIs, which may reflect their larger sample space compared to positive and negative phases.

Buginyanya stands out as the only ZARDI in which the average-of-extremes exceeds the absolute SPEI value of 2.0, crossing thresholds for both extreme wetness and dryness. By contrast, Bulindi and Abi do not frequently experience severe dryness, , as their average dry extremes (SPEI minima) remain within the range (-0.5, -1.5).

3.3 Correlation Analysis Between IOD and SPEI

3.3.1 Correlation Patterns During IOD Phases

During a positive IOD phase, correlations between the DMI and SPEI indicate how moisture conditions respond to increasingly positive DMI values. A positive correlation implies wetter seasons with stronger positive IOD, while a negative correlation suggests drier conditions.

Under negative IOD phases, the interpretation differs. A positive correlation signals drier outcomes during stronger negative IOD conditions. Conversely, a negative correlation suggests that stronger negative IOD conditions correspond to higher SPEI values, indicating wetter conditions.

3.3.2 Interaction Between IOD and ENSO Cycles

IOD phases often coincide with ENSO cycles, raising the possibility of compound effects. For instance, positive IOD phases have coincided with El Niño events in 1972, 1982, 1997, 2015, and 2018, while negative IOD phases aligned with La Niña in 1995, 1998, and 2021. To capture this interaction, the analysis distinguishes between four scenarios: pure positive IOD, pure negative IOD, positive IOD with El Niño, and negative IOD with La Niña. Stronger correlations in combined events suggest that ENSO acts as a secondary driver, intensifying moisture extremes. This implies that relying solely on IOD-based triggers may underestimate agricultural risk, highlighting the need to incorporate ENSO signals into index design.

3.3.3 Visualised Interaction Between IOD and ENSO Cycles

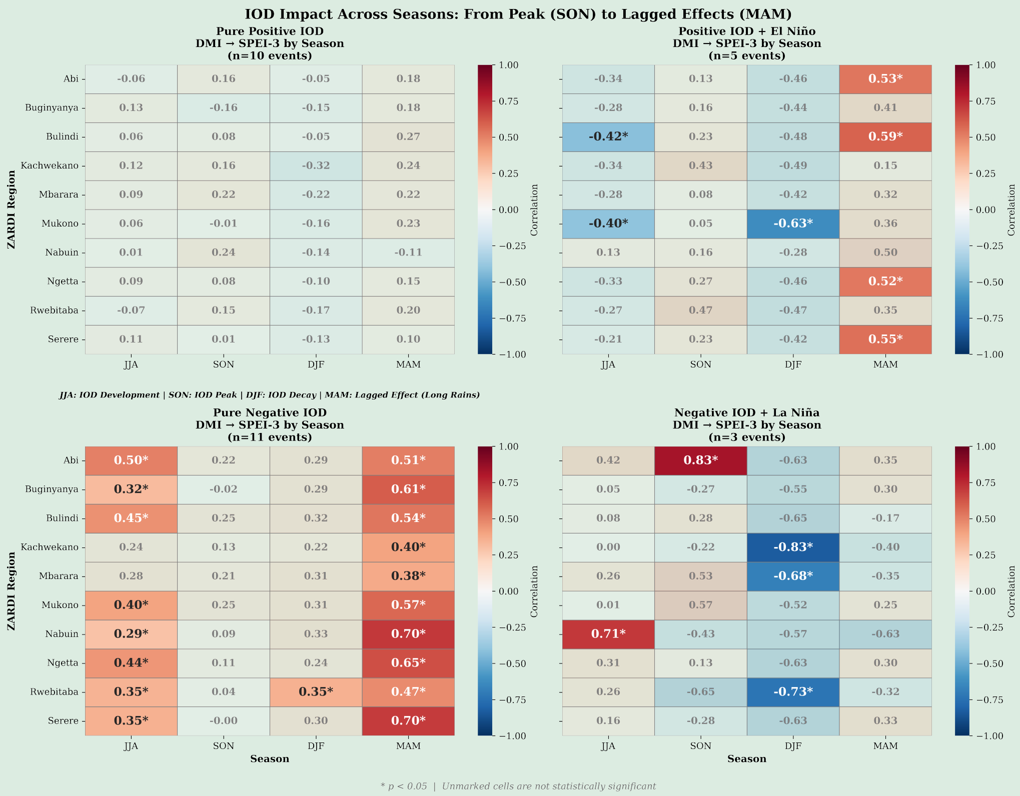

Figure 10: Heatmap of SPEI-IOD correlation values, highlighting shifts in climate signal strength during active ENSO phases

The seasonal dimension – JJA, SON, DJF, MAM – captures the full lifecycle of an IOD event, including its lagged effect on Uganda's long rains. JJA represents the development phase, SON its peak, DJF its decay, and MAM reflects the lagged impacts on the long rains. Extending the analysis window beyond the IOD lifecycle allows the inclusion of the subsequent MAM season, enabling a more comprehensive assessment of delayed climatic effects.

The tables below summarise statistically significant correlations ($p < 0.05$), organised by season and ZARDI across the four IOD–ENSO scenarios.

Table 6: Number of Significant Correlations by Season and Scenario (out of 10 ZARDIs)

Season	Pure Pos IOD	Pos IOD + El Niño	Pure Neg IOD	Neg IOD + La Niña
JJA	0/10	2/10	8/10	1/10
SON	0/10	0/10	0/10	1/10
DJF	0/10	1/10	1/10	3/10
MAM	0/10	4/10	10/10	0/10

Table 7: Significant Season–ZARDI Combinations by Scenario

ZARDI	Pure Pos IOD	Pos IOD + El Niño	Pure Neg IOD	Neg IOD + La Niña
Abi	–	MAM	JJA, MAM	SON
Buginyanya	–	–	JJA, MAM	–
Bulindi	–	JJA, MAM	JJA, MAM	–
Kachwekano	–	–	MAM	DJF
Mbarara	–	–	MAM	DJF
Mukono	–	JJA, DJF	JJA, MAM	–
Nabuin	–	–	JJA, MAM	JJA
Ngetta	–	MAM	JJA, MAM	–
Rwebitaba	–	–	JJA, DJF, MAM	DJF
Serere	–	MAM	JJA, MAM	–

3.3.4 Weaknesses of Pure Positive IOD in Uganda

Analysis of pure positive IOD events reveals no statistically significant relationships across the study period. Correlation values remain consistently weak across all ZARDIs and seasons, with none exceeding ± 0.32. This indicates that positive IOD phases have no meaningful independent influence on SPEI in Uganda and are therefore unsuitable as standalone triggers for agricultural risk.

3.3.5 Amplification of Positive IOD Effects During El Niño Events

When positive IOD phases coincide with El Niño events, statistically significant relationships emerge across seven seasonal instances, indicating that ENSO amplifies the positive IOD signal.

Mukono and Bulindi exhibit stronger negative correlations in JJA (-0.40 and -0.42 respectively), with Mukono's signal persisting into DJF (-0.63), suggesting intensified and prolonged drying conditions. In contrast, the MAM season shows statistically significant positive correlations across multiple ZARDIs: Abi ($+0.53$), Bulindi ($+0.59$), Ngetta ($+0.52$), and Serere ($+0.55$).

3.3.6 Impacts of Pure Negative IOD Events on Moisture Patterns in Uganda

Pure negative IOD events produce statistically significant results in two of the four seasons across 80% of Uganda's ZARDIs. Notably, SPEI shows no significant moisture response during SON, despite this season typically marking the peak of IOD activity. MAM exhibits significant relationships across all ten ZARDIs, with correlations ranging from 0.38 to 0.70, suggesting that the IOD signal is strongest during long rains and may operate through lagged climatic effects.

During pure negative IOD episodes, significant positive correlations are observed across eight ZARDIs in JJA and across all ten in MAM. SON and DJF show consistently weak and statistically insignificant relationships.

3.3.7 Effects of Negative IOD Coinciding with La Niña

When negative IOD coincides with La Niña, the moisture response changes noticeably. Only five statistically significant results are observed, compared with twenty-nine under pure negative IOD conditions. Most notably, the number of significant results falls from 10 to 0 in MAM and from 8 to 1 in JJA, suggesting that La Niña weakens the negative IOD signal (though this may also reflect the smaller sample size of three combined events).

Significant results are limited to Abi in SON, Nabuin in JJA, and Kachwekano, Mbarara, and Rwebitaba in DJF. The combined signal also reveals pronounced seasonal reversals. Nabuin shifts from a strong positive correlation during JJA (0.71) to a negative correlation in SON (-0.47). Abi shows a strong positive correlation in SON (0.83), followed by a pronounced negative correlation in DJF (-0.63), suggesting rapid seasonal reversal. More broadly, the strong negative correlations observed in DJF imply wetter-than-expected conditions during what is typically a dry season in Uganda.

3.3.8 Rwebitaba: A Candidate for Negative IOD Index Insurance Triggers

Rwebitaba stands out as the only ZARDI with statistical significance across three seasons during pure negative IOD events, and it also remains significant in DJF when La Niña is present. This consistency makes Rwebitaba the strongest candidate for a negative IOD-based index insurance trigger.

4 Ground-Truthing SPEI with Yield Data

An event coincidence analysis provides a systematic framework for identifying and quantifying the relationships between large-scale climate oscillations, severe weather events (SPEI < -1.5 or SPEI $> +1.5$), and negative shocks to staple crop yields.

At the national level, a severe event is recorded when at least 50% of districts simultaneously exceed the thresholds of -1.5 (severe drought) and $+1.5$ (severe wetness) within the MAM or SON planting season. ENSO events are identified using the RONI, with El Niño and La Niña defined as periods in which values exceed ± 0.5 for five consecutive months. IOD events are identified using the DMI, with phases defined as values exceeding ± 0.4 for three consecutive months within a June–November period.

To isolate the effects of climate from long-term technological advancements, crop yields are detrended using LOWESS (Locally Weighted Scatterplot Smoothing). Residuals (*observed yield - LOWESS trend*) are converted into Z-scores. A year is classified as a low-yield year when the anomaly falls below -1.0 standard deviations (SD) for drought conditions or below -1.5 SD (severe wetness conditions). The stricter wetness threshold is used to account for more acute collapses associated with flooding.

A compound event is therefore defined as a year in which large-scale climate oscillations, severe drought or wetness, and low crop yields occur simultaneously. Statistical significance is verified using both Fisher's Exact Test and a permutation test with 10,000 reshuffles.

Table 8: Years of Severe Drought or Wetness with Coinciding Climate Events

Year	ENSO State	IOD State	Coinciding Events	Condition
1961	Neutral	+IOD	None	Severe Drought
1963	El Niño	Neutral	None	Severe Drought
1964	La Niña	−IOD	La Niña and Negative IOD	Severe Drought
1968	Neutral	−IOD	None	Severe Drought
1971	La Niña	−IOD	Compound Event (Maize)	Severe Drought
1972	El Niño	+IOD	El Niño and Positive IOD	Severe Drought
1975	La Niña	Neutral	None	Severe Drought
1997	El Niño	+IOD	Compound events (Millet, Cassava, Sorghum)	Severe Wetness
2000	La Niña	Neutral	None	Severe Wetness
2002	El Niño	Neutral	None	Severe Wetness
2007	Neutral	Neutral	None	Severe Wetness
2012	Neutral	+IOD	None	Severe Wetness
2015	El Niño	Neutral	None	Severe Wetness
2016	La Niña	−IOD	La Niña and Negative IOD	Severe Wetness
2017	La Niña	Neutral	None	Severe Wetness
2019	Neutral	+IOD	Compound event (Maize)	Severe Wetness
2021	Neutral	Neutral	None	Severe Wetness
2023	El Niño	+IOD	El Niño and Positive IOD	Severe Wetness

The analysis of severe droughts identifies one compound case in 1971 affecting millet. A prolonged period of crop stress is observed between 2003 and 2009, specifically affecting maize and beans. In contrast, cassava performed strongly between 2000 and 2007, with yield anomalies exceeding $+2.0$, indicating greater resilience. In recent years,

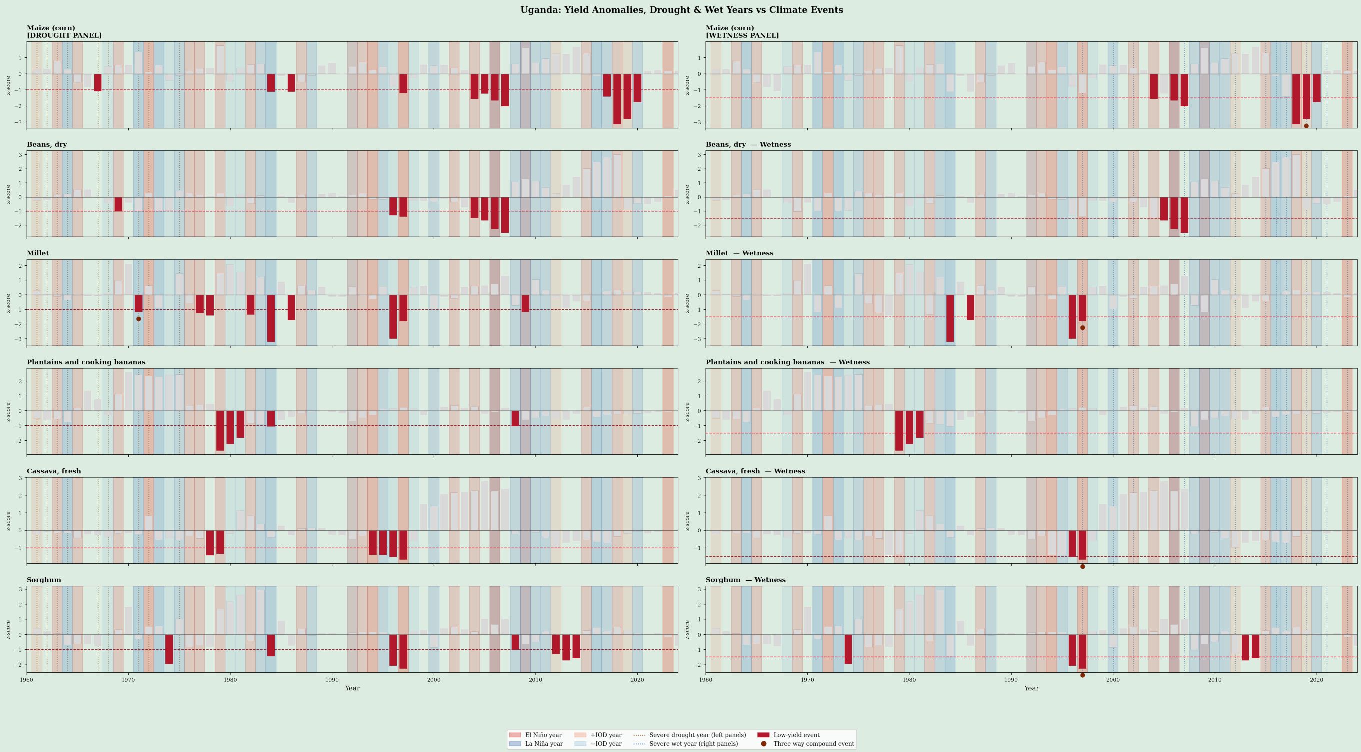

Figure 11: Yield Anomalies and Climate event coincidence with Dry vs Wet Years

maize and sorghum have exhibited increased volatility, with maize recording severe negative anomalies ($z < -2.0$) in 2018–2019. Crops such as cassava, plantains, and cooking bananas demonstrate greater resistance to national drought, with no recorded crop failures during severe drought years.

This resilience is partially explained by spatial distribution. Cassava and plantains are predominantly grown in higher-rainfall regions such as Mukono and Buginyanya. On the other hand, maize and millet are concentrated in drier zones such as Nabuin, Bulindi, and Abi, where lower rainfall and higher temperatures increase the risk of drought.

Analysis of severe wetness events reveals a different pattern. The coincidence of El Niño and a positive IOD phase in 1997 stands out as a catastrophic year, with widespread crop failures affecting millet, sorghum, and cassava. Since 1997, the frequency of severe wetness has increased across Uganda. Maize emerges again as the most vulnerable crop. By contrast, plantains and cooking bananas show strong resilience to severe wetness.

Wetness-related crop failures tend to be more concentrated in single years, such as 1997, indicating that severely wet events trigger simultaneous failures across multiple staple crop types. Overall, compared to drought, severe wetness poses a higher risk to Uganda's food basket, as it produces more synchronised crop losses.

5 Insurance Design Implications

This section translates the preceding findings into policy and insurance recommendations.

5.1 Trigger Design by ZARDI

A trigger is the objective condition that activates a payout under a parametric insurance policy. In this report, SPEI derived from NOAA or CCKP weather data supports three practical trigger structures:

Wetness Trigger. A payout is activated when SPEI exceeds $+1.5$, indicating severe wetness associated with heavy rainfall, waterlogging, and potential crop damage.

Drought Trigger. A payout occurs when SPEI falls below -1.5, signalling severe drought conditions characterised by prolonged rainfall shortages and heat stress.

Dual Trigger. Payouts are activated for either extreme: SPEI exceeds $+1.5$ (wetness) or falls below -1.5 (drought). Best suited to ZARDIs with increasing climate volatility.

5.1.1 ZARDIs Warranting a Dual Trigger

Eastern and central ZARDIs such as Buginyanya, Mukono, Bulindi, and Serere exhibit high variability and frequent extreme events, making them well-suited to dual-trigger insurance products.

Buginyanya stands out as the most volatile region. It is the only ZARDI in which the average of extremes exceeds an absolute SPEI threshold of ± 2.0 under both positive and negative IOD phases. In the 2020s, its distribution extends below -2.0 and above +2.5, indicating simultaneous exposure to severe drought and wetness. With a precipitation coefficient of variation exceeding 64%, it experiences the highest interannual variability.

Mukono has experienced a sharp rise in volatility, from 18.4% in the 2010s to 39% in the 2020s, with the highest SPEI outliers among all ZARDIs. It is also the only region showing significant negative correlations under combined positive IOD and El Niño in both JJA (-0.4) and DJF (-0.63), indicating harsher conditions in dry seasons.

Bulindi shows a strong upward trend in volatility, from 19.8% in the 2010s to 31.7% in the 2020s. Under positive IOD combined with El Niño, Bulindi shows a significant negative correlation in JJA (-0.47), followed by a strong positive correlation in MAM (0.59), indicating sharp seasonal reversals.

Serere displays pronounced expansion in variability during the 2015–2016 El Niño, alongside high severity levels. It shows a significant positive correlation in MAM (0.55) under positive IOD and El Niño conditions, and has experienced 7–8 extreme MAM events per decade since 2000.

5.1.2 ZARDIs Warranting a Drought Trigger

Northern ZARDIs, Nabuin, Ngetta, and Abi, show consistent indicators of drought risk, making them suitable for primarily drought-based insurance triggers.

Nabuin exhibits the strongest decreasing trend in rainfall onset during MAM $(\tau = -0.217)$. As a unimodal rainfall region, delayed onset can have severe consequences for crop yields. Under the combined negative IOD and La Niña scenario, it displays a strong positive correlation in JJA (0.71), indicating a drying pattern.

Ngetta also shows a significant decline in MAM onset $(\tau = -0.158)$. Under pure negative IOD conditions, it records a strong positive correlation in MAM (0.65), indicative of drying pressure during the primary planting season.

Abi presents a slightly mixed risk profile. It shows a strong positive correlation under negative IOD combined with La Niña during SON (0.83), indicating severe drying conditions during planting. However, its median SPEI has drifted towards wetter conditions over time, and a significant positive correlation in MAM (0.53) under positive IOD and El Niño suggests some exposure to wetness risk as well.

5.1.3 ZARDIs Warranting a Wetness Trigger

Western regions, particularly Mbarara and Kachwekano, show increasing wetness trends, supporting the use of primarily wetness-based triggers.

Mbarara has historically recorded lower rainfall peaks (150–180mm), yet recent decades show a pronounced increase in wetness risk. Since 2000, the region has experienced 8–10 extreme MAM wetness events. A strong negative correlation (-0.68) in DJF under negative IOD and La Niña conditions indicates increasing wetness even in typically dry months.

Kachwekano, despite having the lowest volatility, shows a strong negative correlation (-0.83) in DJF under negative IOD combined with La Niña, suggesting increased wetness during normally dry periods, which can elevate SPEI values ahead of the MAM planting season.

5.1.4 Overall Vulnerability

Across all regions, certain ZARDIs emerge as particularly vulnerable due to their exposure to multiple climate risks.

Buginyanya is the most exposed, characterised by a high coefficient of variation (64%), pronounced lower-tail drought risk despite rising median SPEI, and the only case where both extreme drought and wetness (± 2.0) occur in the average-of-extremes analysis during IOD events.

Mukono shows high vulnerability, with the highest recorded El Niño severity in both the 2015–2016 event and the 2020s (39%), the most pronounced upward shift in median SPEI, and significant bidirectional correlations during positive IOD combined with El Niño. It also exhibits the steepest increase in volatility among all ZARDIs.

Nabuin presents a distinct risk profile. It consistently appears as a drought outlier, shows the strongest declining trend in rainfall onset, and lacks a fallback planting season due to its unimodal rainfall regime.

5.2 Dynamic Model Design

Traditional pricing approaches based on historical loss tables or burn rates are becoming increasingly unreliable under climate change. This section introduces a dynamic modelling framework that utilises SPEI as a responsive, self-updating, and forward-looking trigger for insurance design.

Model Architecture

Layer 1 – Set up the baseline period.

Track A: *Quantile Delta Mapping (QDM) for tail estimation.* Using the structural break at approximately 2000, QDM harmonises the pre-2000 record onto the post-2000 quantile structure. This produces a full 1950–2023 series whose extreme quantiles reflect current climate magnitudes rather than the blended 73-year average.

Track B: *Rolling window for annual trigger recalibration.* Each year, the trigger is recalculated using the most recent 20–25-year window of SPEI data rather than the full historical record. This track identifies the threshold used as the trigger for the next season.

Layer 2 – Calculate conditional probabilities.

Technique A: *IOD/ENSO conditional probability tables.* For each ZARDI, season, and climate driver combination, the empirical probability that SPEI crosses the trigger threshold is computed. The output is a table comprising the pre-season risk signals, relevant for Horizon 1.

Technique B: *Logistic regression for continuous probability scoring.* Using lagged climate drivers (DMI observed in JJA and RONI in the prior season), the binary outcome of whether SPEI crosses the trigger threshold in the upcoming MAM or SON season is predicted.

Technique C: *Copula modelling for coincident event tails.* When sample sizes of coincident events are small, a bivariate copula models the joint tail dependence between the DMI and RONI without requiring the full co-occurrence record. Given the expected lower-tail dependence on coinciding climate drivers, a Clayton copula is more appropriate.

Layer 3 – Forward Risk Projection.

Horizon 1: Seasonal pre-warning (3–6 months). At the start of JJA each year, the Australian Bureau of Meteorology and NOAA CPC provide probabilistic DMI and RONI forecasts, and ICPAC is ingested for the Greater Horn of Africa seasonal outlook. These forecasts are propagated through the conditional probability tables, yielding a ZARDI-level trigger probability for the upcoming SON or MAM season.

Retrospective validation is available within the existing dataset. For each year, JJA-observed DMI and RONI are used as a proxy for the seasonal forecast. The conditional probability table is applied, and the resulting seasonal outlook is compared to the actual SPEI outcome, giving a hindcast skill score (e.g. Brier Skill Score).

Horizon 2: Monthly in-season monitoring. SPEI is updated monthly as new precipitation and temperature data arrive during an active season. A trajectory-based alert occurs when the current SPEI is in the warning zone. Required data can be sourced from monthly CHIRPS actuals, ERA5-Land, or the World Bank CCKP API updates.

Horizon 3: Sub-seasonal crop-stage monitoring. Using sub-seasonal forecast products such as CHIRPS-GEFS to monitor SPEI trajectory during agronomically critical growth stages, this horizon helps understand where moisture stress has the greatest impact. This requires switching the timescale from 3 to 1 for SPEI calculations to resolve the 15-day signals of CHIRPS-GEFS.

Layer 4 – Dynamic Recalibration and Basis Risk Scoring.

Technique A: *Rolling event coincidence analysis.* Re-runs annually as new FAOSTAT yield data and SPEI actual values arrive.

Technique B: *Basis risk scoring.* Type 1 basis risk is where a trigger is met without a significant yield loss (insurer overpays). Type 2 basis risk is where significant yield loss occurs without a trigger being met (farmer unprotected).

Technique C: *Quantile Regression for trigger boundary uncertainty.* This gives a confidence band, mitigating the uncertainty that a single threshold would give in a non-stationary climate. Important for regulatory documentation and auditability.

6 Adaptation Strategies

This section translates the preceding empirical findings into actionable recommendations for institutional design and data frameworks.

Genetic Selection for Anaerobic Stress

Crop breeding strategies should pivot from prioritising drought tolerance to enhancing tolerance to waterlogging. This includes selecting cultivars capable of maintaining metabolic function under oxygen-depleted, saturated soil conditions, which are becoming increasingly prevalent.

Pricing Implications of Non-Stationarity

Traditional pricing strategies based on historical loss tables are becoming increasingly unreliable in a non-stationary climate. Dynamic pricing models, such as those incorporating rolling calibration windows, are better suited to capturing evolving risk patterns and adjusting to rapid, climate-driven changes in geographic risk profiles.

6.1 Institutional, Policy, and Data Infrastructure Recommendations

Establish a National Agricultural Climate Risk Registry.

The findings throughout this report demonstrate that climate risk in Uganda is spatially heterogeneous and non-stationary. A national registry jointly updated by the Ministry of Finance & Ministry of Agriculture (MAAIF), Uganda Bureau of Statistics (UBOS), and the Uganda Meteorology Authority should record SPEI anomalies, ENSO and IOD event classifications, and crop yield data at the ZARDI level on an annual basis. This registry would serve as a shared foundation for insurance pricing, government disaster response, and development finance.

Adopt SPEI as the Standard Index for Agricultural Insurance Products in Uganda.

The Uganda Insurers Association (UIA), in collaboration with MAAIF, should formally adopt SPEI as the reference index for agricultural parametric insurance triggers in Uganda, superseding single-variable thresholds such as rainfall thresholds. SPEI captures the combined effect of precipitation deficits and elevated heat stress. For instance, rainfall-only triggers would not be activated during a drought year driven by heat stress despite normal rainfall, leaving farmers underinsured. The standardised normal nature of SPEI indicates that its statistical properties are consistent across each ZARDI, regardless of their differing rainfall patterns. A SPEI value of -1.5 reflects the same moisture stress in Buginyanya as it does in Mbarara, regardless of their differing rainfall patterns. Rainfall thresholds calibrated for one zone would be either too conservative or permissive for the other, creating systematic pricing misrepresentations across the portfolio.

Integrate IOD and ENSO Signals into Seasonal Agricultural Advisory.

Publicly available seasonal outlooks from the IGAD Climate Prediction and Applications Centre (ICPAC), the National Oceanic and Atmospheric Administration Climate Prediction Centre (NOAA CPC), and the Australian Bureau of Meteorology (BoM) include probability updates that can be utilised between June and August (JJA) to aid planting decisions before the MAM long rains. Seasonal planting guidance should be distributed to farmers with explicit reference to ZARDI-level risk elevations associated with IOD and ENSO indices. For instance, when NOAA CPC signals an emerging El Niño and BoM simultaneously forecasts a positive IOD phase, farmers in regions such as Ngetta, Serere, Bulindi, and Abi should be advised to prepare for severe wetness during the upcoming MAM season.

Establish a Multi-Source Data Integration Pipeline for Operational Trigger Monitoring.

Near-real-time SPEI monitoring requires a pipeline that ingests monthly CHIRPS precipitation actuals and ERA5-Land temperature data, computes SPEI at the district level, and aggregates these values to the ZARDI level within 5–10 days after each month's end. These outputs can be shared with UAIS-licensed insurers. For forward-looking seasonal risk assessments, the probabilistic forecasts from ICPAC, the Australian Bureau of Meteorology, and NOAA can be formally ingested into the same pipeline, enabling the Horizon 1 seasonal pre-warning described in section 5.2.

7 Conclusion

The evidence assembled across 73 years of SPEI data, FAOSTAT crop yields, and global climate oscillation indices converges on three key inferences. First, the country has experienced a measurable shift from a drought-dominated climate before 2000 to one increasingly characterised by extreme wetness, particularly affecting the MAM season.

Second, this transition is spatially uneven. Eastern and central ZARDIs are experiencing rising exposure to both drought and excess rainfall, while northern regions remain predominantly drought prone. These asymmetries make a single, national insurance pricing model both inefficient and inequitable.

Third, the Indian Ocean Dipole emerges as a robust pre-season indicator of moisture anomalies, with strong correlations between the Dipole Mode Index and SPEI, particularly during the MAM season under negative IOD conditions.

Taken together, these findings support the basis for differentiated, dynamically calibrated parametric insurance products anchored to SPEI rather than simpler rainfall proxies. Such products require integration with seasonal climate forecasts, standardised data systems, and ongoing monitoring of basis risk. The institutional and product architecture outlined in section 6 provides a framework for developing a climate risk market that is credible, adaptive, and financially sustainable under increasingly non-stationary conditions.

Potential Stakeholders

Policy & Finance. Ministry of Finance & Ministry of Agriculture (MAAIF): They want to identify, develop, and incentivise the adoption of climate-smart agricultural technologies and management practices that contribute to climate adaptation of agricultural value chains to sustainably increase productivity and household incomes while enhancing resilience to climatic shocks.

Uganda Insurers Association (UIA) & Banks: Insurance companies need this framework to set more accurate premiums. Banks feel safer lending money to farmers if the farm is insured, as the loans are de-risked.

Development & Implementation (World Bank, FAO, USAID): They are currently shifting from handout programs toward sustainability programs. The Sahel Climate Catastrophe Layer (SCCL), piloted by the World Food Programme in 2024, shows this. This data provides the evidence they need to fund insurance subsidies.

Agribusiness Cooperatives: Large-scale farmer groups need to understand the ongoing climate trends to decide which crops require investment into drought- or wetness-resistant varieties.

A Methodology

A.1 Rainfall Onset Data Preparation and Trend Analysis

Data preparation. Monthly SPEI values are averaged across duplicate districts within each ZARDI, representing a singular value per ZARDI per month per year.

Cumulative SPEI onset detection. SPEI values are summed forward from February (for MAM) or August (for SON). Onset occurs when the cumulative sum first exceeds $+0.5$ within March–June (MAM) or September–December (SON). Years without threshold crossing are labelled as no onset, affecting the sample size per ZARDI.

Mann-Kendall trend test with autocorrelation correction. Each ZARDI's annual onset series is tested using the Mann-Kendall test. If lag-1 autocorrelation exceeds 0.1, the Hamed-Rao variant is used; otherwise, the standard test applies. Significance is set at $\alpha = 0.05$ over the whole period.

Sen's slope is calculated for each ZARDI, providing a median-based estimate of the magnitude of the onset trend, resistant to outlier effects.

A.2 Correlating DMI and SPEI

To investigate the relationship between the IOD and weather conditions at each ZARDI, the Dipole Mode Index (DMI) is correlated with SPEI. Because one variable is unitless (SPEI) and the other is in °C (DMI), their absolute magnitudes cannot be compared, so statistical association rather than direct arithmetic operations is required. DMI and SPEI values are aggregated as monthly means for each ZARDI and season.

The Spearman Rank correlation method is employed because it does not require the assumption of a linear relationship and is suitable for non-normal distributions:

$$\rho = \frac{1 - 6\sum d^2}{n(n^2 - 1)}$$

A strong correlation is present when two variables move together consistently, characterised by a correlation coefficient between ± 0.5 and ± 1.0. Correlation does not imply causation.

B Data Validation

Before analysis, each data source was subjected to systematic quality checks.

B.1 Climate Data (SPEI, Precipitation, Temperature)

Monthly precipitation and mean surface air temperature series sourced from the World Bank Climate Change Knowledge Portal (CCKP) were inspected for completeness across the full 1950–2023 study period. Any district-month observation missing across more than 5% of the full record was flagged and excluded from months where the gap occurred rather than imputed, to avoid introducing artificial smoothing into the tails of the distribution. No ZARDI lost any contributing district observation because of this procedure.

Outlier screening was applied using a rolling 10-year interquartile range filter. Monthly values exceeding five times the local IQR above the 75th percentile or below the 25th percentile were flagged for manual inspection. Values confirmed as physically plausible were retained; values inconsistent with the surrounding record were removed and treated as missing.

SPEI values were derived using the Thornthwaite method for Potential Evapotranspiration estimation, with latitude inputs sourced at the district level. The resulting SPEI series were cross-checked against published SPEI-3 outputs from the Global SPEI Database (SPEIbase) for the corresponding grid cells to confirm directional consistency.

B.2 Climate Index Data (DMI and RONI)

Dipole Mode Index values were sourced from NOAA PSL and cross-referenced against the Japan Meteorological Agency DMI archive. IOD events were classified as positive or negative only when the DMI exceeded ± 0.4 for three or more consecutive months within the June–November window. Any year in which the two source archives disagreed on the event phase for a given month was treated as ambiguous and excluded from the IOD phase panels.

Relative Oceanic Niño Index (RONI) values were sourced from NOAA CPC and validated against ONI for the overlapping period. El Niño and La Niña events were classified using the ± 0.5 threshold sustained across five consecutive months.

B.3 Crop Yield Data (FAOSTAT)

National-level annual crop yield series for the six staple crops were downloaded from FAOSTAT. Series continuity was assessed by inspecting year-on-year changes exceeding three standard deviations of the full-record distribution. Two breaks were identified in the cassava series and one in the millet series; these years are flagged in the coincidence analysis output.

LOWESS detrending was applied with a bandwidth parameter of 0.4. The residual z-scores were inspected for autocorrelation using the Durbin-Watson statistic; where significant first-order autocorrelation was detected, the effective sample size used in Fisher's Exact significance test was adjusted downward accordingly.

B.4 Dynamic Model Validation

Hindcast Validation (Layer 2). A leave-one-out hindcast over 1980–2023 evaluates predictive performance using post-regime-shift data. Performance is measured using the Brier Skill Score (BSS) against a climatological baseline defined by post-2000 exceedance frequencies. Calibration is assessed using reliability diagrams.

Regime Consistency Check (Layer 1). QDM is validated by comparing the adjusted pre-2000 distribution with observed post-2000 quantiles using Q-Q plots. Rolling 20–25-year recalibration is tested against fixed historical thresholds; sustained divergence (> 0.25 SPEI units over three years) signals potential structural change requiring review.

Basis Risk Validation (Layer 4). Trigger outcomes are compared with detrended yield z-scores to compute Type 1 (false payout) and Type 2 (missed loss) basis risk rates, disaggregated by ZARDI, crop, and trigger type. Where Type 2 risk is elevated, quantile regression defines a confidence band around trigger thresholds. Annual recalibration ensures responsiveness, with rates above 20% triggering formal review.

C References

SPEI Information. https://climatedataguide.ucar.edu/climate-data/standardized-precipitation-evapotranspiration-index-spei

Citizen Report (Source of district latitude Information) https://thecitizenreport.ug/wp-content/uploads/2022/05/all-district-cordinates.csv

Nabuin (Karamoja) unimodal rainfall patterns. https://www.fao.org/giews/countrybrief/country.jsp?code=UGA

Paulo, A.A., Rosa, R.D., and Pereira, L.S.: Climate trends and behaviour of drought indices based on precipitation and evapotranspiration in Portugal. *Nat. Hazards Earth Syst. Sci.*, 12, 1481–1491, https://doi.org/10.5194/nhess-12-1481-2012, 2012.

Agricultural Risk Assessment Study 2015. https://parm.org/document/agricultural-risk-assessment-study-in-uganda/

World Bank Climate Risk Country Profile: Uganda. https://reliefweb.int/report/uganda/climate-risk-country-profile-uganda

MacLeod, D., and C. Caminade, 2019: The Moderate Impact of the 2015 El Niño over East Africa and Its Representation in Seasonal Reforecasts. *J. Climate*, 32, 7989–8001, https://doi.org/10.1175/JCLI-D-19-0201.1

ENSO Information. https://education.nationalgeographic.org/resource/el-nino/

El Niño Southern Africa Impact. https://www.unocha.org/publications/report/mozambique/southern-africa-el-nino-regional-humanitarian-overview-september-2024

RONI classification data. https://ggweather.com/enso/roni.htm

Malteser International El Nino information. https://www.malteser-international.org/en/current-issues/natural-disasters/el-nino.html

ZARDI Information: NARO. https://naro.go.ug/zardis/

Relative Oceanic Niño Index. https://www.cpc.ncep.noaa.gov/products/analysis_monitoring/enso/roni/

Indian Ocean Dipole Index data. https://psl.noaa.gov/data/timeseries/month/DMI/

Indian Ocean Dipole event information (Japan Meteorology Association) https://ds.data.jma.go.jp/tcc/tcc/products/elnino/iodevents.html

Indian Ocean Dipole Phases. https://www.bom.gov.au/climate/iod/

MAAIF UCSATP objectives. https://www.agriculture.go.ug/ucsatp/

Parametric Insurance Definition and Case Studies. https://bluemarblemicro.com/parametric-insurance/

SCCL SPEI Insurance case study (West Africa - drought). https://www.preventionweb.net/resource/case-study/world-food-programmes-sahel-climate-catastrophe-layer

ENSO Probabilities from NOAA CPC updated monthly. https://cpc.ncep.noaa.gov/products/analysis_monitoring/enso/roni/probabilities/

DMI Probabilities from Copernicus. https://climate.copernicus.eu/charts/packages/c3s_seasonal/products/c3s_seasonal_plume_mm

DMI Probabilities from BoM. https://www.bom.gov.au/climate/ocean/outlooks/?index=iod

Africa Agricultural Network - Uganda Agricultural Insurance Scheme Report. https://africaagriculturalnetwork.com/how-ugandas-agriculture-insurance-scheme-reached-1-million-farmers/

ZARDI MAP Creation tool (MapChart). https://www.mapchart.net/africa.html

OPM Budget Framework 2022/23. https://budget.finance.go.ug/sites/default/files/Sector%20Spending%20Agency%20Budgets%20and%20Performance/Office%20of%20the%20Prime%20Minister_2.pdf

OPM Strategic Plan 2025–2030. https://opm.go.ug/wp-admin/admin-ajax.php?juwpfisadmin=false&action=wpfd&task=file.download&wpfd_category_id=99&wpfd_file_id=10277&token=&preview=1